Available online at www.sciencedirect.com
ScienceDirect
Journal of Sound and Vibration 305 (2007) 3–21
JOURNAL OF SOUND AND VIBRATION
www.elsevier.com/locate/jsvi

Recent research on identification of moving loads on bridges

L. Yu[a,b], Tommy H.T. Chan[b,c,*]

[a]College of Science and Engineering, Jinan University, Guangzhou 510632, PR China
[b]Department of Civil and Structural Engineering, The Hong Kong Polytechnic University, Hung Hom, Kowloon, Hong Kong, PR China
[c]School of Urban Development, Faculty of Built Environment & Engineering, Queensland University of Technology, GPO Box 2434, Queensland 4001, Australia

Received 14 June 2005; received in revised form 1 March 2007; accepted 2 March 2007
Available online 23 May 2007

Abstract

Identification of moving loads on bridges is an important inverse problem in the civil and structural engineering field. It is an effective way to better understand the interaction between the bridge and vehicles traversing it in order to achieve a satisfactory lifespan for the future bridge design. The study on identification of moving loads has made a big progress over the past years. This paper reviews the current knowledge on factors affecting performance of moving force identification methods under main headings below: background of moving force identification, experimental verification in laboratory and its application in field. It mainly focuses on the potential of four developed identification methods, i.e. Interpretive Method I (IMI), Interpretive Method II (IMII), Time Domain Method (TDM) and Frequency–Time Domain Method (FTDM). Some parameter effects, such as vehicle–bridge parameters, measurement parameters and algorithm parameters, are also discussed. Although there are still many challenges and obstacles to be overcome before these methods can be implemented in practice, some conclusions that have been achieved on moving force identification are highlighted and recommendations served as a good indicator to steer the direction of further work in the field.

1. Introduction

With the increasing advent of heavier and fast vehicles as well as the use of structural forms and materials that permits the bridge to be more slender, accurate and reliable data on the nature and extent of vehicles use of both the road and bridge network, especially dynamic moving vehicle loads, is extremely important for not only the design of bridges and pavements but also their monitoring and retrofitting in the transportation engineering [1]. However, it is difficult to directly measure the interaction forces between the vehicles and a bridge because they are in motion and time varying. Under this circumstance it would be beneficial if the forces could be calculated indirectly using the measured response data of bridges. In the past several decades, a lot of researchers have extensively studied the indirect calculation of forces from measured structural responses data. Stevens [2] has given an excellent survey of the literature on the force identification problem as well as an overview. Dobson and Rider [3] reviewed the work that had been done on force prediction and highlighted those areas that require further research. Olsson [4] intended to give a basic understanding of the

*Corresponding author. Tel.: +852 2766 6061; fax: +852 2334 6389.
E-mail address: cetommy@polyu.edu.hk (T.H.T. Chan).

0022-460X/$ - see front matter © 2007 Elsevier Ltd. All rights reserved.
doi:10.1016/j.jsv.2007.03.057

moving load problem and reference data for more general studies. However, most of the traditional ways to acquire axle load data could only measure static (or equivalent static) axle loads, and they are expensive and subject to bias, e.g. the Weigh-in-Motion systems can only acquire static equivalent axle loads of a vehicle [5–9]. The dynamic load data are valuable because the dynamic wheel loads might increase road surface damage by a factor of 2–4 over that due to static wheel loads [10], the repeated application of moving heavier vehicles directly contribute to fatigue failure and crack propagation in bridge structure, leading to a reduction in useful life. As for the study on identification of dynamic loads, Whittemore et al. [11] and Cantieni [12] have separately described systems that use instrumented vehicles to measure dynamic loads on bridge decks. Unfortunately, the acquired data are also subject to bias.

In the recent years, some great effort has been made for moving force identification from the dynamic responses of bridges. A series of identification methods have been proposed, which can compute dynamic wheel loads with an acceptable accuracy [13]. The first method, the Interpretive Method I (IMI, [14]), developed a system to measure the dynamic vehicle–bridge interaction forces from the bridge total responses caused by the inertial or D'Alembert's forces and the damping forces, in which the bridge deck is modeled as an assembly of lumped masses interconnected by massless elastic beam elements. The second, the Interpretive Method II (IMII, [15]), was similar to IMI but used Euler-Bernoulli beam model for the bridge deck in the interpretation of dynamic loads crossing the deck. The Euler-Bernoulli beam theory together with modal analysis was used to identify moving loads from the bridge responses. The third, the Time Domain Method (TDM, [16]), modeled the bridge deck as a simply supported Euler-Bernoulli beam with viscous damping and the vehicle/bridge interaction forces was modeled as one-point or two-point loads with fixed axle spacing, moving at constant speed. The moving forces were then identified using the modal superposition principle in time domain. Further, the Frequency–Time Domain Method (FTDM, [17]) performed Fourier transformation on the equations of motion which are expressed in modal co-ordinates. The relation between the responses and the moving forces was established first and the force spectrums were calculated by the least-square method in the frequency. The time histories of the moving forces can then be obtained by performing the inverse Fourier transformation. These above-mentioned methods have been enhanced and merged into a Moving Force Identification System (MFIS) [13]. The MFIS has been shown to be a successful identification system and the identification methods involved in the MFIS could be accepted as practical methods with higher identification accuracy to some extent [13,18,19]. However, there still exist some limitations if these methods involved in the system could actually be operated in practice [20,21]. Some enhancement mode, improvement or further research is required to accommodate them to the application in field.

This paper provides a review on current knowledge of the factors affecting the performance of moving force identification methods proposed primarily by the authors as well as their collaborators in this area. It aims at evaluating the potential of the above-mentioned four methods involved in the MFIS based on the experimental verification in laboratory and its application in field. Some parametric effects are also discussed, and some conclusions on moving force identification drawn and further research in need highlighted finally.

2. Background of moving force identification

2.1. Models

2.1.1. Models of bridge–vehicle system

In practice, the bridge–vehicle system is a very complicated system. The interaction between the bridge and the vehicle is a complex phenomenon governed by a large number of different parameters. The use of simplified models is more effective to establish a clear connection between the governing parameters and the bridge response than a complex model. Normally, the bridge decks are modeled as beams (Euler-Bernoulli beam or Timoshenko beam) or plates (isotropic plates or orthotropic plates) and vehicles are modeled as a moving force, a moving mass or a moving oscillator for simple analysis of vehicle interaction.

2.1.2. Models of bridges

There are two kinds of models of bridges in the MFIS. One is the *Beam-Element Model* [14] in which a bridge can be modeled as an assembly of lumped masses interconnected by massless elastic beam elements.

The total modal responses, $[R]_{\text{total}}$, on the bridge equal to the equivalent static responses, $[R]_{\text{static}}$, caused by the external loads less the responses caused by the inertia forces, $[R]_{\text{inertia}}$, and the damping forces, $[R]_{\text{damping}}$, or equivalently as

$$[R]_{\text{total}} = [R]_{\text{static}} - [R]_{\text{inertia}} - [R]_{\text{damping}}. \tag{1}$$

The other model is the *Continuous Beam Model* [13], assuming a Timoshenko beam [22] of constant cross-section with constant mass per unit length, having linear, viscous proportional damping and with small deflections. From there follow three special cases: If the effect of rotatory inertia is neglected and only the effect of shear on the dynamic deflection of the beam is considered, it is called a shear beam. If the effect of shear is neglected and only the effect of rotatory inertia is considered, the so-called Rayleigh beam model results. If both the effect of shear and the effect of rotatory inertia are neglected, the classical Euler-Bernoulli beam model is obtained. In most problems encountered in practice the effects of rotatory inertia and shear can safely be neglected with little error (Euler-Bernoulli beam); however, for short, deep beams with height-span ratios larger than about 1/10 or beams made of materials sensitive to shear stresses, it is desirable to give consideration to the effect of shear and rotatory inertia [1].

If the bridge model is considered as a simply supported Euler-Bernoulli beam with a span length L, constant flexural stiffness EI, constant mass per unit length ρ and viscous proportional damping C, the equation of motion when the force P moves from left to right at a speed c can be expressed as [20,21]

$$\rho\frac{\partial^2 v(x,t)}{\partial t^2} + C\frac{\partial v(x,t)}{\partial t} + \mathrm{EI}\frac{\partial^4 v(x,t)}{\partial x^4} = \delta(x-ct)P(t), \tag{2}$$

where $v(x,t)$ is the beam deflection at point x and time t and $\delta(x-ct)$ is the Dirac delta function. Based on modal superposition, the solution of Eq. (2) can be expressed as follows:

$$v(x,t) = \sum_{n=1}^{\infty} \sin\frac{n\pi x}{L} q_n(t), \tag{3}$$

where $q_n(t)$ is the nth modal displacement. After substituting Eq. (3) into Eq. (2), integrating the resultant equation and using both the boundary conditions and the properties of $\delta(t)$, the equation can be expressed in terms of $q_n(t)$ as follows:

$$\ddot{q}_n(t) + 2\xi_n\omega_n\dot{q}(t) + \omega_n^2 q_n(t) = \frac{2}{\rho L}p_n(t) \quad (n = 1, 2, \ldots, \infty), \tag{4}$$

where

$$\omega_n = \frac{n^2\pi^2}{L^2}\sqrt{\frac{\mathrm{EI}}{\rho}}, \quad \xi_n = \frac{C}{2\rho\,\omega_n}, \quad p_n(t) = P(t)\,\sin\left(\frac{n\pi\bar{x}}{L}\right) \tag{5}$$

are the nth modal frequency, the modal damping and the modal force, respectively. The distance of the axle from the left-hand support is denoted by $\bar{x}$. In the moving force identification problem, the unknown time-varying force $P(t)$ is identified from the structural responses.

2.1.3. Models of vehicles

For the case of low moving speed or low mass ratio, the simple moving force model can be a good approximation to the complex moving mass problem [1]. For the case of a high mass ratio and a high moving speed, the moving force model cannot be applied, and the complicated time-variant system analysis for the moving mass problem must be conducted to ensure an accurate investigation [23–26]. If a softly sprung vehicle traverses a flexible structure, the interaction effects become very important, and the moving oscillator model should be adopted as it is more realistic in some engineering applications [27–29]. Usually, a quarter-truck model, a half-single-unit two-axle truck model, and a half five-axle semi-trailer truck model developed by Todd and Kulakowski [30], or three-dimensional (3D), 2D, and single sprung mass (1D) system [31] are adopted.

2.2. Theoretical background

A series of identification methods are proposed and emerged into a MFIS, which include four methods in determining the dynamic axle loads from bridge responses caused by the travelling vehicles. They are the IMI [14], IMII [15], TDM [16], and FTDM [17], respectively. The first method is based on a *Beam-Element Model*, the others are based on a continuous beam model.

2.2.1. Interpretive Method I (IMI)

It is used to measure the dynamic axle loads acting on a bridge, which is modeled as an assembly of lumped masses interconnected by massless elastic beam elements. The IMI reconstructs the loads from the measured bridge responses caused by the inertial or D'Alembert's forces and the damping forces. The nodal responses for displacements or/and bending moments at any instant are given by Eqs. (6) and (7), respectively

$$\{Y\} = [Y_A]\{P\} - [Y_I][\Delta m]\{\ddot{Y}\} - [Y_I][C]\{\dot{Y}\}, \tag{6}$$

$$\{M\} = [M_A]\{P\} - [M_I][\Delta m]\{\ddot{Y}\} - [M_I][C]\{\dot{Y}\}, \tag{7}$$

where $[\Delta m]$ is the diagonal matrix containing values of lumped mass; $[C]$ is the damping matrix; $[Y_A]$, $[Y_I]$ are matrices for nodal forces to obtain nodal displacements, and $[M_A]$, $[M_I]$ are matrices for nodal forces to obtain nodal bending moments. The vector of the axle loads, $\{P\}$, can be identified using any one of the bridge responses, such as bending moments $\{M\}$, displacements $\{Y\}$, velocities $\{\dot{Y}\}$ or accelerations $\{\ddot{Y}\}$ measured.

2.2.2. Interpretive Method II (IMII)

This method is similar to IMI but uses Euler-Benoulli beam model for the bridge deck in the interpretation of dynamic loads crossing the deck. If there are k moving loads with the same speed c on the bridge, Eq. (4) can be written as

$$\begin{Bmatrix} \ddot{q}_1 \\ \ddot{q}_2 \\ \vdots \\ \ddot{q}_n \end{Bmatrix} + \begin{Bmatrix} 2\xi_1\omega_1\dot{q}_1 \\ 2\xi_2\omega_2\dot{q}_2 \\ \vdots \\ 2\xi_n\omega_n\dot{q}_n \end{Bmatrix} + \begin{Bmatrix} \omega_1^2 q_1 \\ \omega_2^2 q_2 \\ \vdots \\ \omega_n^2 q_n \end{Bmatrix}$$
$$= \frac{2}{\rho L} \begin{bmatrix} \sin\dfrac{\pi(ct-\hat{x}_1)}{L} & \sin\dfrac{\pi(ct-\hat{x}_2)}{L} & \cdots & \sin\dfrac{\pi(ct-\hat{x}_k)}{L} \\ \sin\dfrac{2\pi(ct-\hat{x}_1)}{L} & \sin\dfrac{2\pi(ct-\hat{x}_2)}{L} & \cdots & \sin\dfrac{2\pi(ct-\hat{x}_k)}{L} \\ \vdots & \vdots & \vdots & \vdots \\ \sin\dfrac{n\pi(ct-\hat{x}_1)}{L} & \sin\dfrac{n\pi(ct-\hat{x}_2)}{L} & \cdots & \sin\dfrac{n\pi(ct-\hat{x}_k)}{L} \end{bmatrix} \begin{Bmatrix} P_1 \\ P_2 \\ \vdots \\ P_k \end{Bmatrix}. \tag{8}$$

At first the bridge responses at various locations such as the vertical displacements or bending moments are transformed to modal values. The central difference method is used to numerically differentiate the modal displacements to obtain the corresponding modal velocities and modal accelerations. Then the above equation becomes a set of linear equations in which the values of the axle load at any instant, i.e. $\{P_1, P_2, \ldots, P_k\}$, can be solved by the least -squares method.

2.2.3. Time Domain Method (TDM)

Eq. (4) can be solved in the time domain by the convolution integral and the dynamic deflection $v(x,t)$ of the beam at point x and time t can be obtained as

$$v(x,t)=\sum_{n=1}^{\infty}\frac{2}{\rho L\omega_n'}\sin\frac{n\pi ct}{L}\int_0^t \mathrm{e}^{-\xi_n\omega_n(t-\tau)}\sin\,\omega_n'(t-\tau)\,\sin\frac{n\pi c\tau}{L}P(\tau)\,\mathrm{d}\tau, \tag{9}$$

where $\omega_n'=\omega_n\sqrt{1-\xi_n^2}$. Because both the time-varying force $P(t)$ and the response $v(x,t)$ are step functions in a small time interval Δt, Eq. (9) can be rewritten in discrete terms and rearranged into a set of linear equations, $P(t)$ can then be solved by the least-squares method in time domain.

2.2.4. Frequency–Time Domain Method (FTDM)

Eq. (4) can also be solved in the frequency domain using the Fourier Transform of both Eqs. (3) and (4). The Fourier Transform of the dynamic deflection $v(x,t)$, i.e. Eq. (3) is

$$V(x,\omega)=\sum_{n=1}^{\infty}\frac{2}{\rho L}\sin\frac{n\pi x}{L}H_n(\omega)P(\omega). \tag{10}$$

Similarly, a set of N-order simultaneous equations can be established in the frequency domain. The force $P(\omega)$ consisting of the real and imaginary parts can be found by solving the N-order linear equations. The time history of the time-varying force $P(t)$ can then be obtained by performing the inverse Fourier transformation.

2.3. Solutions

As mentioned above, it is easy to find that most of the identification methods are eventually converted to a linear algebraic equation set below:

$$Ax=b, \tag{11}$$

where $x\in R^n$ is the time series vector of the unknown time-varying force $P(t)$, $b\in R^k$ is the time series vector of the measured response of bridge deck. The system coefficient matrix $A\in R^{k\times n}$ is associated with the bridge–vehicle system. In principle, if $k>n$ Eq. (11) will have a solution given by the least-squares method as

$$x=A^{+}b=[(A^{\mathrm{T}}A)^{-1}A^{\mathrm{T}}]b, \tag{12}$$

where A^{+} denotes the *pseudo-inverse* (PI) of matrix A. The solution vector x is called *PI solution*. This definition requires matrix A to have full rank. If matrix A is close to rank deficient then A^{+} is best calculated from singular value decomposition (SVD) of matrix A [32]. If matrix A is real, the SVD of A is $\mathrm{USV}^{\mathrm{T}}$, its inverse can easily be calculated from $A^{+}=\mathrm{US}^{-1}\mathrm{U}^{\mathrm{T}}$. For simplicity, assuming that matrix A has no exact zero singular values, it can be shown that the least-squares solution vector x is given by

$$x=\sum_{i=1}^{\min(k,n)}\frac{u_i^{\mathrm{T}}b_i}{\sigma_i}v_i. \tag{13}$$

The solution vector x here is called *SVD solution*.

3. Experimental verification in laboratory

In order to evaluate the moving force identification methods and to conduct a comparative study, a series of experiments have been carried out in laboratory. After having designed and constructed different vehicle models, such as two-axle vehicle models and multi-axle vehicle models, and different bridge models, such as simply supported bridge models, continuous beams and plate bridge models, the correctness and efficiency of methods are evaluated and the effects of various parameters on the identification process were studied [13].

As an example, a simply supported beam with a span of 3.678 m long and 101 mm × 25 mm uniform cross-section was constructed. It was made from a solid rectangular mild steel bar with a density of 7335 kg/m^3 and a flexural stiffness EI = 29.92 kN/m^2. Two model cars were made in the laboratory to simulate two-axle vehicle

and multi-axle vehicle respectively. One has two axles at a spacing of 0.55 m and was mounted on four rubber wheels. The static mass of the whole car was 12.1 kg in which the mass of rear axle was 3.825 kg, its axle spacing to span ratio (ASSR) is 0.15. The other has three axles according to the American Association of State Highway and Transportation [33] loading code, set two types of ASSR, 0.15:0.15 and 0.15:0.20, respectively. Its axle load ratio of 1:4:4 and 3:7:7 W are adopted in the experiments. Combined weight of the model car, $W = 2$ kg for case 1:4:4 W and $W = 1$ kg for 3:7:7 W are set for test. The total weight of car is 18 kg for case 1:4:4 W and 17 kg for case 3:7:7 W, respectively.

The model car was pulled by a string wound on the drive wheel of an electric motor in the front of the beam. Its speed can be adjusted to control and determine the car speed exactly. When the car moved across the beam bridge, the induced bridge responses were recorded simultaneously using strain gauges and accelerometers installed on the lower surface of the beam. If these measured responses are input into the MFIS, any method in the system can be selected to identify the moving axle loads, which are subsequently used to reconstruct the so-called "rebuilt" responses of bridge. The relative error percentage (RPE) between the measured and rebuild responses are adopted to assess the efficiency and robustness of identification methods. If it is a simulation case, the RPE data between the real and identified forces are also used to assess the identification methods selected.

3.1. Evaluation of identification methods

Under the same conditions, Table 1 gives a comparison between RPE values when the four identification methods are used to estimate the two moving axle loads from measured bending moments at seven measurement stations, here, L denotes the beam span length. All the RPE data are lower than 10% except at the first station ($L/8$) and seventh station ($7L/8$) for IMII method. This illustrates that all the four identification methods involved in the MFIS are correct and effective. However, the results from both TDM and FTDM are clearly better than those from both IMI and IMII. Further, the results provided by SVD solution are better than ones by PI solution, particularly for FTDM. It shows SVD technique can improve the identification accuracy.

3.2. Effects of parameters on identification accuracy

Many parameters influence the moving force identification problem and it is necessary to study their effects on the identification methods. Some effects of the main parameters, such as bridge–vehicle parameters, measurement parameters and algorithm parameters, are reported here.

3.2.1. Effects of bridge–vehicle parameters

3.2.1.1. Bridge mode numbers. Usually, a sufficient number of vibration modes of bridge must be involved in the identification calculation. But, what is the sufficient number of modes? The answer depends not only on

Table 1
Comparison of identified results by various methods

Method	RPE (%)						
	Sta. 1	Sta. 2	Sta. 3	Sta. 4	Sta. 5	Sta. 6	Sta. 7
IMI	9.37	9.51	9.73	9.62	9.55	9.14	8.36
IMII	12.2	6.00	6.98	4.40	6.05	5.75	13.2
TDM	5.42	3.08	1.80	2.58	1.95	3.44	4.83
	5.43	3.09	1.80	2.56	1.94	3.43	4.83
FTDM	5.74	2.80	2.15	2.08	2.14	2.41	4.74
	4.53	2.52	1.87	1.95	1.82	2.24	3.17

Notes: The underlined values are from SVD solution, others from PI solution, same meanings below.

Table 2
Effect of mode number (MN)

Method	MN	RPE (%)						
		Sta. 1	Sta. 2	Sta. 3	Sta. 4	Sta. 5	Sta. 6	Sta. 7
IMII	2	94.91	57.80	54.02	55.24	56.97	63.63	97.00
	3	5.84	5.08	5.32	4.92	5.08	4.95	5.67
	4	6.19	5.07	5.34	4.91	5.01	4.82	5.97
TDM	3	***	***	***	***	***	***	***
	4	5.80	3.32	1.89	2.86	1.98	3.77	5.75
	5	5.42	3.08	1.80	2.58	1.95	3.44	4.83
FTDM	3	****	****	****	****	****	****	****
	4	13.58	7.19	5.69	5.93	5.55	6.75	12.91
	5	5.74	2.80	2.15	2.08	2.14	2.41	4.74

Notes: Symbols '***' and '****' represent RPE values larger than 100% and 1000%, respectively.

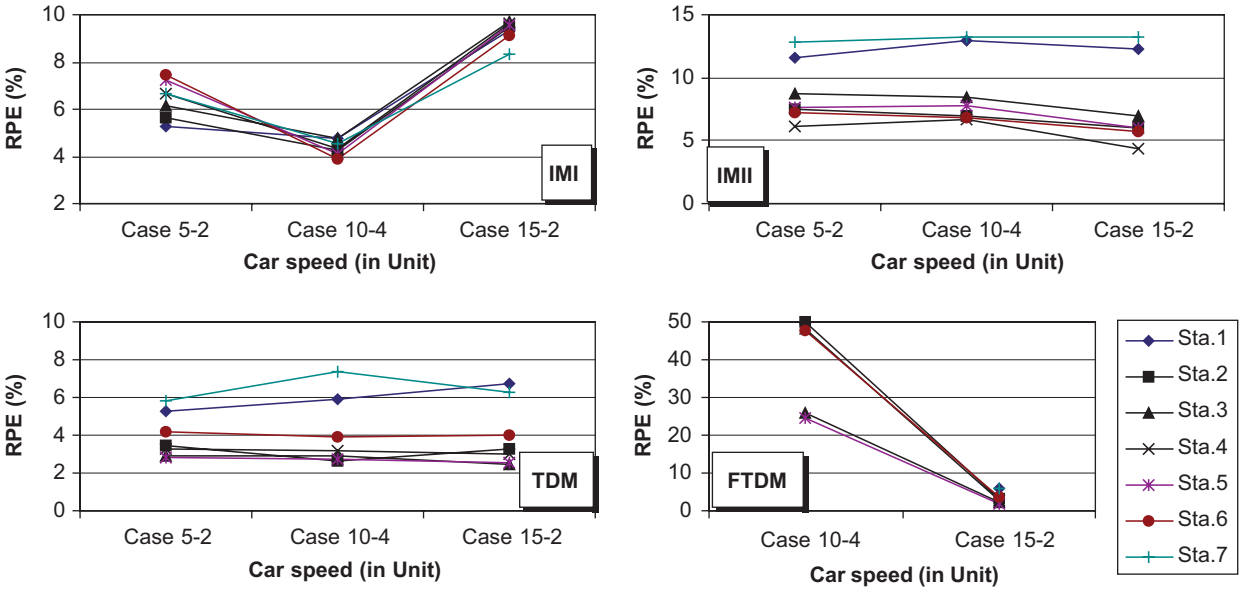

Fig. 1. Effect of car speed.

the characteristics of the bridge–vehicle system but also on the solution to the over-determined equation used in the moving force identification method. The IMI is independent of the mode number and not included here. Table 2 gives the evaluation on the effect of mode number (MN). It shows that the IMII needs at least the first three modes or more to correctly identify the two moving forces. For both the TDM and FTDM, the minimal necessary mode number required is 4. If the first five modes are used to identify the two moving forces, the identification accuracy is the highest in the cases studied [20,21]. Generally, the mode number involved should be more than or at least equal to one more than axle numbers of vehicle [34].

3.2.1.2. Vehicle speed. Vehicle speed plays an important role in the dynamic behavior of a bridge subjected to loads moving across the bridge [4,25,35]. Fig. 1 illustrates the effect of speeds on the identification methods. It is interesting to notice that the RPE values first decrease and then increase with increasing vehicle speed for the IMI. But the change in the RPE values is not so significant although decreasing slightly with increasing vehicle speed for both IMII and TDM. It may be concluded that both IMII and TDM are independent of vehicle speeds. Anyway, the IMII is more suitable for the higher vehicle speed. The TDM can effectively

identify the forces in all the speed cases. A faster vehicle speed is also of benefit to both the TDM and FTDM, and unfortunately, the FTDM fails in the lower speed cases if PI solution is used to solve the equations [34]. However, when using the SVD solution the situation is completely changed. It makes the FTDM from original ineffective to effective although it also shows the FTDM has a better identification accuracy in the fast speed as listed in Table 3 [18]. This is because the coefficient matrix of the equation is often rank deficient or nearly rank deficient due to noise or uncertainty in the measured data. In this situation, the best way to calculate the pseudo-inverse is via the SVD technique for coefficient matrix.

3.2.1.3. Axle spacing to span ratio (ASSR). Setting ASSR range between 0.2 and 0.05, Table 4 lists some of RPE data between the real and identified moving forces with various ASSRs. Results of the representative studies show errors larger than 10% are obtained for IMI at and below the ASSR of 0.12. For IMII, the errors also increase with a smaller ASSR. However, it is shown that acceptable results can be obtained for values as small as 0.05. For TDM and FTDM, the results show that there is no adverse effect by reducing the ASSR. The corresponding RPE errors are found to be zero all the time. This implies that the accuracy of identified forces using both methods is not dependent on the ASSR [34].

3.2.1.4. Vehicle frame. Heavy vehicles mainly include two kinds of frames, articulated and nonarticulated vehicle frames, respectively. Previous research using analytical model has shown that nonarticulated vehicles generate much higher vibration on the bridge compared to articulated vehicles [56]. Therefore, in order to study the influence of different vehicle frames on the bridge behaviors and on the identification accuracy, the three-axle vehicle models were allowed to switch from articulated to rigid connection, i.e. nonarticulated connection between tractor and the semi-trailer by two fixed studs in the laboratory [19]. Fig. 2 illustrates a comparison of identified moving forces between the articulated and the nonarticulated vehicles. Obviously, the

Table 3
Comparison of effect of vehicle speeds on FTDM

Speed case	Solutions	RPE (%)						
		Sta. 1	Sta. 2	Sta. 3	Sta. 4	Sta. 5	Sta. 6	Sta. 7
5–2	PI	fail	fail	fail	fail	fail	fail	fail
	SVD	23.71	13.00	6.79	7.90	6.93	12.40	26.37
10–4	PI	***	50.0	25.9	48.2	24.8	47.6	***
	SVD	23.3	12.6	7.99	8.32	7.79	11.8	26.3
15–2	PI	5.94	3.29	2.05	2.66	2.01	3.57	5.89
	SVD	5.87	3.24	2.04	2.65	1.98	3.55	5.84

Table 4
Summary of RPE data between real and identified forces with ASSRs

ASSR	RPE (%)							
	IMI		IMII		TDM		FTDM	
	Axle 1	Axle 2	Axle 1	Axle 2	Axle 1	Axle 2	Axle 1	Axle 2
0.20	0.444	0.205	0.650	0.392	0.0	0.0	0.0	0.0
0.15	0.681	0.252	0.689	0.345	0.0	0.0	0.0	0.0
0.12	231.3	45.0	0.702	0.311	0.0	0.0	0.0	0.0
0.10	342.1	105.5	0.723	0.306	0.0	0.0	0.0	0.0
0.09	N/A	N/A	0.804	0.278	0.0	0.0	0.0	0.0
0.05	N/A	N/A	1.358	0.539	0.0	0.0	0.0	0.0

identified moving forces are feasible and acceptable for the articulated vehicle. For the nonarticulated vehicle, the identified moving forces at the first and the third axle are greater than their corresponding static axle loads, i.e. 20 and 80 N, respectively, this is because the second axle was hanging in the air as the vehicle moved into the middle of the span due to the large deflection of the main beam by weight itself. However, their summation is equal to the total static weight of vehicle. It shows that the identified forces at the first and the third axels are correct and gross weight is really distributed to the first and third axles. The above results show that the identified multi-axle vehicle loads are reasonable and acceptable for both the articulated and nonarticulated vehicles. The MFIS can correctly identify the multi-axle vehicle loads even if the middle axle of the nonarticulated vehicles is hanging in the air.

3.2.1.5. Vehicle suspension system. In an attempt to assess the influence of a vehicle suspension system on the bridge dynamic behavior and on identification accuracy, three types of suspension systems are incorporated in the vehicle models. They are rigid connection (Fig. 3(a)), sprung connection (Fig. 3(b)), and pre-compressed sprung connection (Fig. 3(c)) between vehicle frame and axle, respectively to simulate different suspension systems as illustrated in Fig. 3. Table 5 shows that the suspension systems make an obvious impact on both dynamic characteristics of vehicles and identification accuracy. The fundamental frequency of a vehicle is significantly changed by the suspension system. It is evidently beneficial to the improvement of identification accuracy when the nonarticulated vehicles are suspended and provided with more suspension systems [19]. On

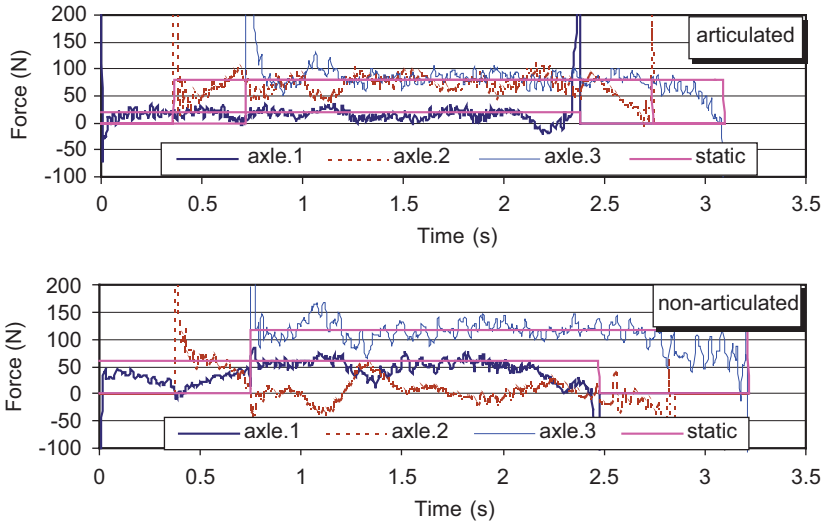

Fig. 2. Identified loads by FTDM for non- and articulated vehicles (20:80:80 N).

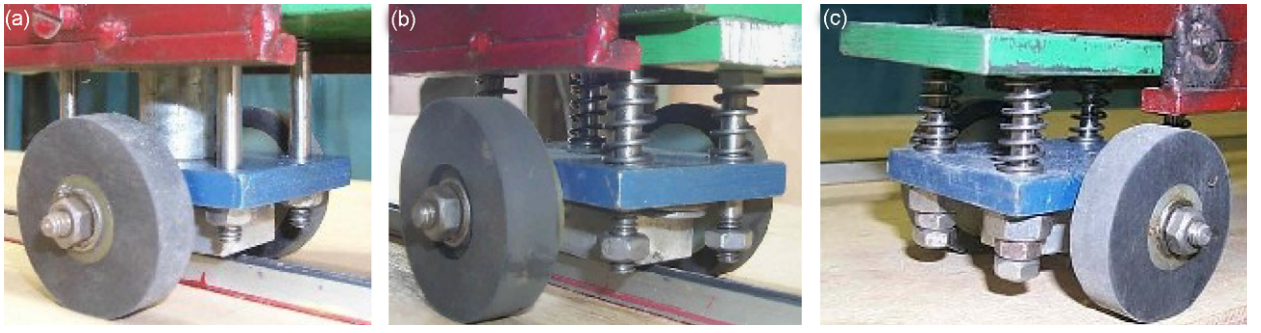

Fig. 3. Three different suspension systems mounted in laboratory.

Table 5
Comparison of identified results under different suspension systems

Vehicle description	Method	RPE (%)					
		Sta. 1	Sta. 2	Sta. 4	Sta. 5	Sta. 6	Sta. 7
(1) 288NA*, 31.27 Hz	TDM	5.86	6.38	4.45	4.31	5.06	9.82
Rigid connection	FTDM	14.0	8.04	6.90	6.48	7.80	16.9
(2) 288NAS3, 30.20 Hz	TDM	4.85	5.34	3.55	3.08	3.96	6.82
Suspended at third axle	FTDM	4.33	5.00	3.15	3.07	4.25	7.06
(3) 288NAS23, 14.15 Hz	TDM	4.45	4.47	3.25	3.09	3.13	4.99
Suspended at both second and third axles	FTDM	3.90	3.88	2.69	3.03	3.53	4.65
(4) 288NAP3, 10.97 Hz	TDM	7.86	5.62	3.20	2.75	2.85	5.23
Suspended at both second and third axles	FTDM	4.11	5.04	2.75	2.61	2.90	4.56
(5) E288NAP3, 8.53 Hz	TDM	6.99	15.1	8.10	6.14	4.53	11.8
Suspended at both second and third axles	FTDM	6.41	15.4	7.54	6.33	5.04	11.4
(6) E288NA, 31.38 Hz	TDM	5.74	5.62	3.74	3.32	3.85	6.37
Rigid connection	FTDM	14.7	7.38	5.60	6.13	6.58	16.0

Notes: (1) "E" indicates extended frame vehicle; (2) "S" suspended axle; (3) "NA" non-articulated vehicle; (4) "288" axle weight = 20:80:80 N; (5) "P" pre-compressed by 1 cm at third axle and suspended at both second and third axle.

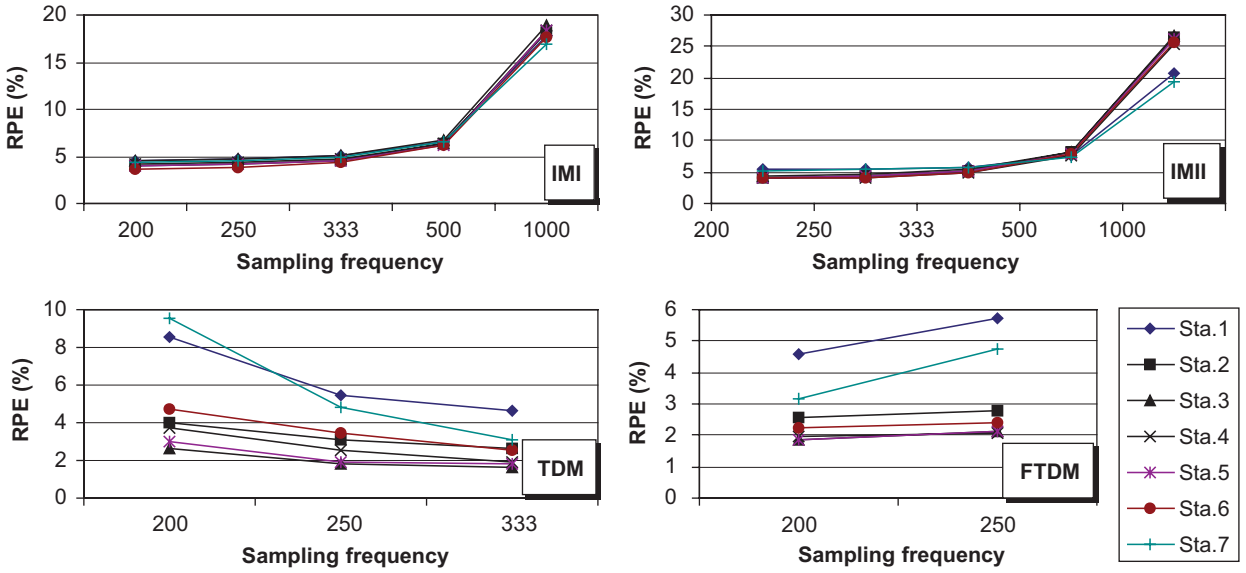

Fig. 4. Effect of sampling frequency using PI.

the other hand, it indicates that the rigid connection gives higher impact to bridges than the other sprung connections between the frame and axle.

3.2.2. *Effect of measurement parameters*

3.2.2.1. Sampling frequency. Fig. 4 gives the effect of sampling frequency on the identification methods. It shows that the effects of sampling frequency using the IMI and IMII are insignificant within 333 Hz, but after this range, the effects become more significant, especially for sampling frequency 1000 Hz, both the IMI and IMII fail. The TDM is suitable for the higher sampling frequency and it has the highest identification accuracy when the highest sampling frequency 333 Hz is employed. The effect of sampling frequency on the FTDM increases with the sampling frequency, and the FTDM fails if the sampling frequency is equal to or higher than 333 Hz and PI solution is used [34]. However, the SVD identified results are clearly different from those

Table 6
Effect of sampling frequencies on FTDM

Sampling frequency	RPE (%)						
	Sta. 1	Sta. 2	Sta. 3	Sta. 4	Sta. 5	Sta. 6	Sta. 7
333 Hz	204.8	168.6	156.8	148.0	153.6	161.9	186.9
	4.51	2.53	1.87	1.95	1.82	2.25	3.17
250 Hz	5.74	2.80	2.15	2.08	2.14	2.41	4.74
	4.53	2.52	1.87	1.95	1.82	2.24	3.17

Table 7
Effect of measurement stations

Method	Total number	RPE (%)						
		Sta. 1	Sta. 2	Sta. 3	Sta. 4	Sta. 5	Sta. 6	Sta. 7
TDM	3	⊗	⊗	15.76	13.39	8.33	⊗	⊗
	4	⊗	1.48	1.44	⊗	1.85	1.56	⊗
	5	⊗	2.17	1.80	2.67	1.94	1.98	⊗
	7	5.42	3.08	1.80	2.58	1.95	3.44	4.83
FTDM	3	⊗	⊗	70.15	77.27	73.90	⊗	⊗
				1.24	1.38	1.05		
	4	⊗	2.90	2.09	⊗	2.11	2.74	⊗
			1.67	1.50		1.51	1.68	
	5	⊗	34.63	17.25	34.68	16.65	32.87	⊗
			2.14	1.71	1.77	1.71	1.63	
	7	5.74	2.80	2.15	2.08	2.14	2.41	4.74
		4.53	2.52	1.87	1.95	1.81	2.24	3.17

Notes: Symbol "⊗" indicates the station is not chosen.

found by PI for the FTDM as listed in Table 6 [18]. The RPE values at each station in Table 6 are almost constant for different sampling frequencies. This means that the identification method is independent of the sampling frequency when adopting the SVD. The SVD can effectively improve the identification accuracy especially when the sampling frequency is of the highest value of 333 Hz set up in the study. The use of the SVD not only makes the identification method effective but also results in good identified results with higher accuracy, whereas direct calculation of the PI solution causes the identification method to fail. Moreover, both the TDM and FTDM have higher identification accuracy than both the IMI and IMII.

3.2.2.2. Measurement stations measurement errors. The effects of sensors on IMI and IMII can be found in Refs. [14,15], respectively and the required numbers of stations can be determined as indicated. For the TDM and FTDM, Table 7 gives the RPE values for different measurement stations. The results show that TDM requires at least three, and at best four, measurement stations to obtain the two correct moving forces. However, the FTDM should have at least one more measurement station than using the TDM, i.e., 4 to obtain the same number of moving forces. Unfortunately, the RPE values are increased obviously when the measurement station total number is equal to 5 for the FTDM. This is because the addition of the fifth station is placed on the $1/2L$ point, namely the node of the second and fourth modes of the simply supported beam. Nevertheless, when the total number of measurement station is equal to 7, which means two more stations are put at the $1/8L$ and $7/8L$, respectively, the RPE values by the FTDM recover normal level to within 10%. It indicates that the FTDM is sensitive to the locations of measuring station, which should be selected carefully when the PI solution is adopted [20,21]. Once the SVD is used for the FTDM, the RPE data, as listed on the

underlined values in Table 7, which show that the identified results are acceptable and they achieve a very high accuracy even though they exceed the acceptable accuracy range when using the PI solution in all the study cases. In particular, the RPE data are less than 2.53% at the middle five stations. It is predicted that the identification method is independent of the measurement stations if the SVD method is adopted [18]. In general, the identification accuracy is better if more measuring stations are adopted for both the TDM and FTDM, but it will take longer computational time.

3.2.2.3. Measurement errors. There are measurement errors for both the laboratory experiments and the field tests of the bridge–vehicle system, for example, vehicle speed error, axle spacing error or location error of measuring sensors. Speeds are possibly the most difficult to be correctly measured because the speeds of vehicles vary significantly with traffic conditions as well as with individual drivers. The study shows that only TDM gives acceptable results when errors exist in the vehicle speed estimation. Speed errors affect the accuracy of identified forces and will also affect indirectly the calculation of axle spacing. If errors in axle spacing are involved in force identification, results show that IMI is the best method for obtaining a higher accuracy of identified forces, and FTDM is the worst method. If sensor location measurement errors occur, TDM will be the least sensitive method, FTDM becomes second and IMI the last. As measurement errors may exist in more than one parameter, a study of the effect of measurement errors in combination shows that TDM and FTDM are the best and worst methods, respectively [34,36].

3.2.3. Effect of algorithm parameters

3.2.3.1. Executing CPU time. Both IMI and IMII take only a few minutes in the force identification calculation for any set of study cases; it is not significant in a measurement of the computational time. However, there exists a different situation for both TDM and FTDM. Each of them consists of three parts, i.e. forming the system coefficient matrix A in Eq. (11), solving the equation and producing the rebuilt responses, respectively. Because FTDM takes three times longer than TDM in forming matrix A, the TDM takes a shorter total time to perform identification than the FTDM [20,21]. In addition, although SVD technique can obviously improve the identification accuracy, especially for FTDM, it increases executive time by 60% when compared to that for the PI solution [18]. It is too expensive and not beneficial to the real-time analysis in situ.

3.2.3.2. Tolerance parameter ε. The SVD computation is usually performed in two stages. In the first stage, matrix A is reduced to an upper bi-diagonal matrix using the Householder transformation. The second stage is an iterative process. It applies a variant of the QR algorithm to reduce the super-diagonal elements to a negligible size and to result in a diagonal form through an iteration procedure. Here ε is a given tolerance parameter as well as a criterion related to rejecting or accepting zero singular values. This criterion may depend on the accuracy of the expected results and, in practice, may be difficult to establish. Fig. 5 illustrates the effect of the tolerance parameter ε on the RPE data. Results show that a smaller tolerance parameter ε is beneficial to moving force identification; the RPE data are constant, say 2.52%, if ε is equal to or smaller than 1.0e−4. However, if ε is too small the computation cost (CPU) is higher because it need more iterations for convergence. To account for all the above aspects simultaneously, a value of ε of 1.0e−6 is appropriate for the case studies [18].

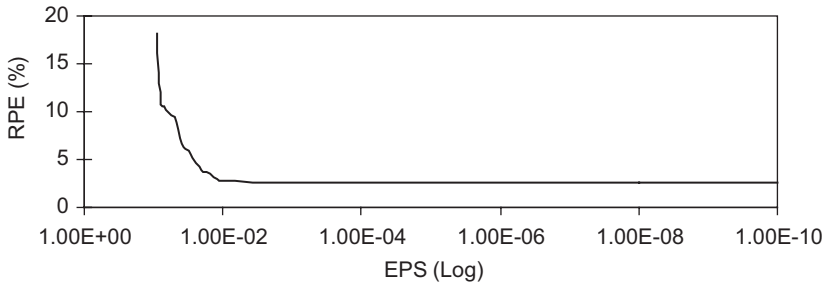

Fig. 5. Effect of tolerance parameter ε (EPS) used in the SVD technique.

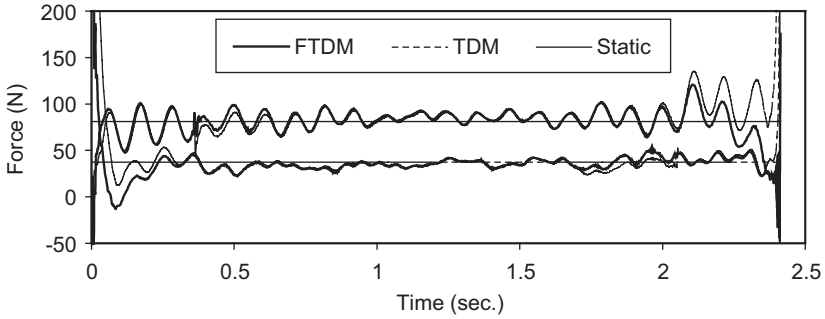

Fig. 6. Identified forces by FTDM and TDM using SVD.

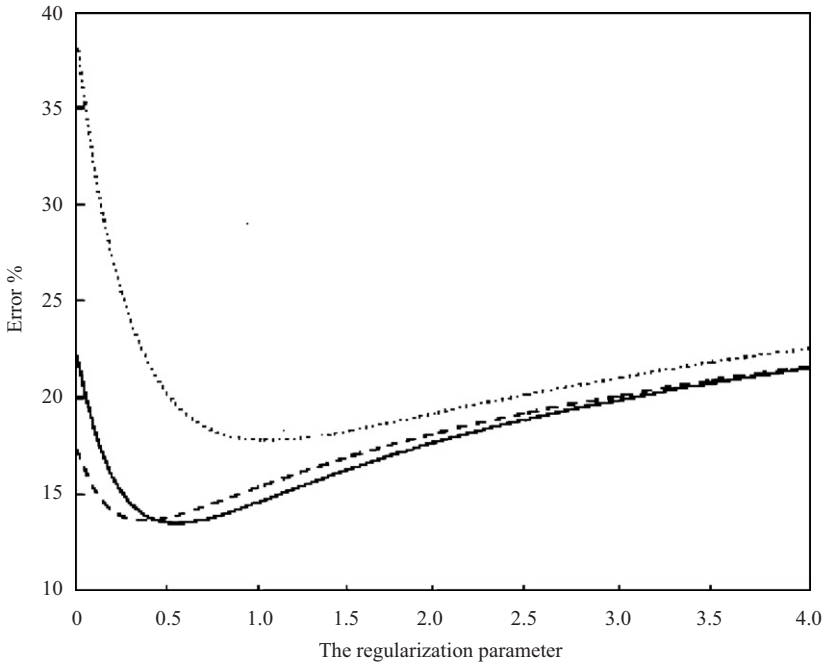

Fig. 7. Typical *S*-curve.

3.2.3.3. Bound parameter λ. The identified results from all the above methods are noise sensitive and they exhibit fluctuations at the beginning and end of the time histories as illustrated in Fig. 6 [37]. These moments correspond to the switching of free vibration state of the structure to the forced vibration state, and vice versa, and the solutions are ill conditioned. A regularization method developed by Tikhonov and Arsenin [38] can be introduced to provide bounds to the solution [39]. However, the difficulty of applying the Tikhonov regularization lies in the method to find the optimal regularization parameter λ. Two effective methods to find the parameter λ are the *S*-curve method [40] and *L*-curve method [41], respectively. Figs. 7 and 8 illustrate the typical *S*- and *L*-curves for different noise levels in the measurement data, respectively. The *S*-curve is a plot of the relative percentage errors between the real and the identified forces against the regularization parameter λ. It is noted from Fig. 7 that the optimal value of λ corresponds to the smallest error. However, the *L*-curve is a plot of the semi-norm of the solution against the residual norm. The norm of residuals E for Eq. (11) is calculated as

$$E = ||[A]\{x\}^{\text{identify}} - \{b\}|| \tag{14}$$

and the first-order regularization proposed by Busby and Trujillo [40], the semi-norm of the estimated forces $\{x\}$ is

$$E1 = \left\| \{x\}_{j+1}^{\text{identify}} - \{x\}_{j}^{\text{identify}} \right\|, \tag{15}$$

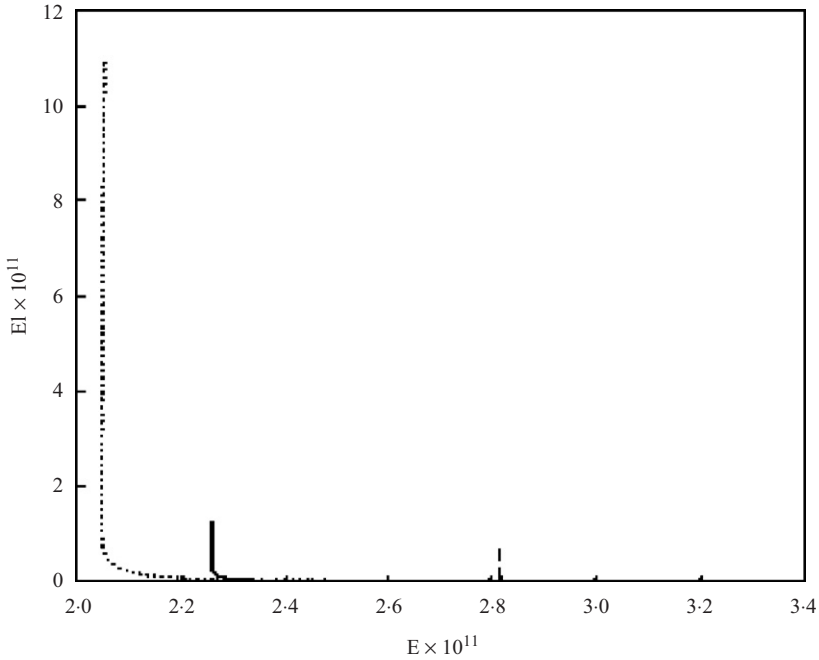

Fig. 8. Typical L-curve.

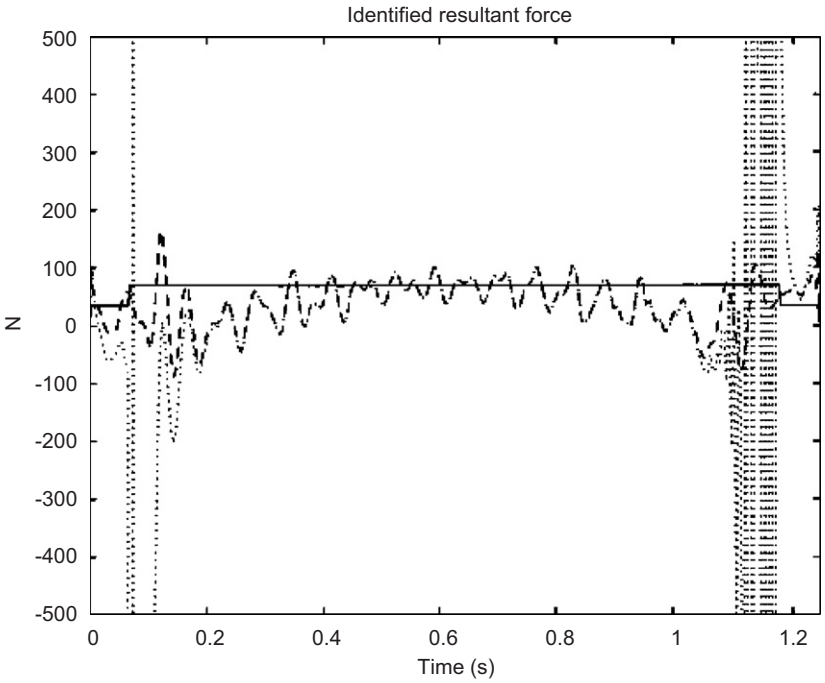

Fig. 9. Comparison of identified resultant forces from laboratory experiments for TDM.

where $\{x\}_j^{\text{identify}}$, $\{x\}_{j+1}^{\text{identify}}$ are the identified forces with λ_j and λ_{j+1}, respectively. All the typical L-curves in Fig. 8 exhibit a corner in each L-curve. The value of λ that corresponds to the point immediately to the right of the corner is the optimum. Fig. 9 illustrates a comparison of identified forces between with and without regularization, here, the bold dash line is for the identified results with regularization. It shows that the regularization only provides bound to the ill-conditioned solution without any smoothing effect on the measurement noise, and the results obtained are greatly improved over those without regularization with acceptable errors from using different combinations of measured responses. Moreover, the TDM is better than the FTDM in solving for the ill-posed problem. Both simulation and laboratory test results indicate that the total weight of a vehicle can be estimated indirectly using moving force identification methods with some accuracy, at least with FTDM [39].

4. Application in field

Before the field tests, a moving force identification method taking into account the effects of pre-stressing is presented [42] based on IMI method. A two-axle medium lorry is modeled as a set of forces, with their magnitudes either constant or time varying, moving across a bridge model with a span length of 28 m. Results show that the identified forces are identical to input forces only when no noise is added to the simulated bridge responses. The identified forces from responses which include noise are poor, even with a noise level as low as 1%. However, the identification can be greatly improved using a low-pass filter. Results also show that the identified forces are over- and underestimated, respectively, when pre-stressing effects are neglected in the identification and calibration processes. Large RPE data are also obtained when pre-stressing effects are neglected in both processes. Additionally, the RPE data decrease with decreasing pre-stressing forces, and do not change with the magnitude of axle forces and mass per unit length.

As an extension work of above theory, field tests were carried out to verify the proposed method in October 1995 on an existing pre-stressed concrete bridge of Ma Tau Wai Flyover, Hunghom, Kowloon, Hong Kong, PR China [20,21]. The test bridge, Ma Tau Wai Flyover comprises a series of 17 simply supported composite slab-on-girder bridges, each with a reinforced concrete slab on the top of pre-stressed concrete girders. According to drawings provided by the Hong Kong Highways Department, the test span is 28.0 m long between the center of piers and 9.326 m wide. The test bridge deck is supported on five pre-stressed concrete girders. A two-axle heavy vehicle of about 150 kN was hired for the calibration test of the field measurements. A total of 35 strain gauges with seven gauges were installed on each of the five girders to acquire the dynamic bending moments of the test bridge deck while a vehicle passed over the test span. The transverse locations of the seven strain gauges on each girder are 3.215, 6.765, 10.312, 13.866, 17.416, 21.21, and 24.516 m away from the first support of the test span, respectively. Seven channels were used to acquire readings for each transverse location. For each transverse location, five strain gauges were connected in a series circuit to acquire the total bending moment at the corresponding transverse section of the test bridge deck.

The dynamic bending moments of the test bridge deck brought about by both a hired control vehicle and in-service 77 vehicles were acquired at seven locations, respectively. Dynamic axle forces were identified by means of the TDM method. The equivalent static axle loads of the two cases are tabulated in Table 8, which shows that the gross weights of Tests 2 and 3 are acceptable with percentage differences of 3.69% and 0.85%, respectively. After obtaining the identified two-axle forces of the control vehicle, the re-built bending moments can be calculated based on the forward problem, and then the RPE data between the measured and the rebuilt

Table 8
Summary of equivalent static forces identified with considering pre-stressing

Test case	Axle 1		Axle 2		Total	
	Equivalent static force (kN)	Difference (%)	Equivalent static force (kN)	Difference (%)	Gross weight (kN)	Difference (%)
2	65.22	1.97	91.22	4.95	156.44	3.69
3	62.48	−2.31	89.69	3.19	152.17	0.85

Table 9
Summary of RPE between responses for control vehicle

Test case	RPE (%)				
	Ch. 2	Ch. 3	Ch. 4	Ch. 5	Ch. 6
2	2.12	3.13	2.74	9.82	7.31
3	5.87	9.96	3.96	2.38	6.40

Table 10
Summary of RPE between responses for in-service vehicles

Test case	Gross weight (kN)	RPE (%)				
		Ch. 2	Ch. 3	Ch. 4	Ch. 5	Ch. 6
A141	97.52	1.95	0.89	9.77	2.40	⊗
A200	54.29	8.80	9.05	9.97	8.25	4.68
A232	70.23	2.89	2.13	0.46	3.22	0.98
A256	54.77	2.85	4.73	1.36	9.61	3.44
A259	102.21	4.77	3.78	3.81	⊗	9.86

Notes: Symbol "⊗" indicates the station is not chosen.

measured bending responses at each channel can be estimated as listed in Table 9 for the control vehicle. It shows that all the RPE errors are acceptable. As the measured responses can be recovered from the identified forces, the identified dynamic axle loads are therefore valid. Since no information was available for the axle loads of the in-service vehicle, no comparison with axle loads can be made here. The accuracy of identified dynamic axle loads was studied using only RPE between the measured and rebuilt responses. Table 10 lists some of the RPE errors of the in-service vehicles. All the above-identified results show that the axle forces can be identified with acceptable accuracy for both hired control vehicle and in-service vehicles. Therefore the proposed method is valid for identifying dynamic axle forces. Gross weights can be obtained by summing up the equivalent axle load of each axle.

5. Conclusions and recommendations

This paper provides a review on recent advances on identification of moving loads on bridges. The theoretical background of four identification methods as an advanced technique are introduced, two solutions to system equations involved in the MFIS are proposed and compared. Numerical simulations, illustrative examples and comparative studies on the effects of different parameters, such as vehicle–bridge parameters, measurement parameters and algorithm parameters, have been carried out and critically investigated. Bridge–vehicle system models have also been fabricated in the laboratory to validate the correctness and robustness of the proposed methods. Field measurements have also been conducted to assess the applicability of the methods involved in the MFIS in practice. The results show that all four identification methods involved in the MFIS can effectively identify moving axle loads on bridges and can be accepted as practical methods with higher identification accuracy. However, there are still many challenges and obstacles to be overcome before these methods could be implemented in practice. Further studies on the moving force identification are necessary and some recommendations based on experiences and results are:

(1) *More proper laboratory models and more field tests*: Although the moving force identification methods are developed and have been shown to be successful, the work mainly focused on laboratory studies of some simple vehicle–bridge models [43]. More properly designed scale models [27] in laboratory and further field work are necessary and recommended to validate the methods and to accommodate them to practical

bridge–vehicle system in engineering, especially consideration of the practical design of bridges, for instance, the effect of a curved bridge [44], the effect of a skew bridge [45], the effect of an inclined bridge, etc.

(2) *Use of various responses of bridge*: Present research is mainly based on the measured bending moment responses induced by the passage of vehicles on bridges; however, other types of bridge responses, especially for acceleration responses [46,47] are easy to measure and operate, and they should be used to identify the moving loads on bridges. Here, a higher sampling frequency, more measurement stations and mode numbers are recommended to adopt in the identification calculation.

(3) *More effective and faster algorithms*: It is always recommended to use the SVD solution instead of the PI solution, especially for the frequency–time domain method. However, performing a full-SVD is too expensive in practical application. An algorithm to compute a partial SVD may be used instead [48], or replacing the full-SVD by a RRQR factorization [49]. The fast computing method and powerful computer is necessary for real time computation and some techniques of splitting the larger coefficient matrix into smaller sub-matrix are recommended in order to make the computation more cost effective.

(4) *Precise calculation format*: The central difference, Newmark-β and Wilson-θ methods are often used in the moving force identification process, the measurement errors are easy to be amplified and spread abroad. The precise time-step integration technique [50] may be used to establish a calculation format between responses of bridges and moving loads on bridges for more accurate results, especial for both IMI and IMII methods.

(5) *Proper treatment of ill-posed problems in the moving force identification*: Moving force identification from bridge responses is a typical inverse problem tends to be ill conditioned, in which the effects of errors are of major concern. Numerical scaling and regularization techniques are needed to improve ill-conditioned effects [2]. However, finding the optimal regularization parameter λ is the main difficulty of applying the regularization technique. *S*-curve, *L*-curve and GCV methods [51] can be used but with the disadvantage that some involved operators are difficult to obtain, subjected to high computation cost, prior information and researcher's experiences as well. Regularization in ill-posed linear inverse problems may be adjusted by the empirical Bayes approach [52] or adaptive strategy [53].

(6) *Conversion of inverse problem of moving force identification*: Moving force identification from dynamic responses of a bridge can also be converted into a kind of forward problem in the structural dynamics [54], or formulated as a well-posed problem by adopting the concept of the time delay [55]. It is likely a new direction of moving force identification in the future.

(7) *Interpretation of the causes of high dynamic axle loads*: Because the mechanism between a bridge and a vehicle is very complicated, the causes of high dynamic axle loads are still under investigation even though many theoretical and experimental studies have been carried out. After having obtained the dynamic moving loads on bridges through the moving force identification techniques, the results can be used not only to study the causes of high dynamic axle loads, but also to better understand the bridge–vehicle interaction, further to explore the relationship between various bridge and vehicle parameters on the development of high bridge responses. It could be used to identify the characteristics of Bridge-Friendly Vehicles finally as well.

Acknowledgments

The project is supported by National Natural Science Foundation of China (50378009) and The Hong Kong Polytechnic University Postdoctoral Fellowship Research Grants (G-YX25).

References

[1] L. Fryba, *Vibration of Solids and Structures Under Moving Loads*, Thomas Telford Ltd., London, 1999.

[2] K.K. Stevens, Force identification problem—an overview, *Proceedings of SEM Spring Conference on Experimental Mechanics*, Florida, USA, 1987, pp. 838–844.

[3] B.J. Dobson, E. Rider, A review of the indirect calculation of excitation forces form measured structural response data, *Proceedings of Institution of Mechanical Engineers, Part C: Journal of Mechanical Engineering Science* 204 (1990) 69–75.

[4] M. Olsson, On the fundamental moving load problem, *Journal of Sound and Vibration* 145 (2) (1991) 299–307.
[5] C. Koniditsiotis, R. Buckmaster, P. Fraser, Australian highway speed weigh-in-motion—an overview, *Road Transport Technology-4, Proceedings of the Fourth International Symposium on Heavy Vehicle Weights and Dimensions*, University of Michigan, Transportation Research Institute, Ann Arbor, 1995, pp. 143–151.
[6] F. Moses, Weigh-in-motion system using instrumented bridges, *Journal of Transport Engineering, ASCE* 105 (1978) 233–249.
[7] O.K. Norman, R.C. Hopkins, Weighing vehicles in motion, *Public Road* 27 (1) (1952) 1–17.
[8] R.J. Peters, Axway—a system to obtain vehicle axle weights, *Proceedings of 12th ARRB Conference*, Australia, 1984, pp. 19–29.
[9] R.J. Peters, Culway—an unmanned and undetectable high speed vehicle weighing system, *Proceedings of 13th ARRB/Fifth REAAA Conference*, Australia, 1986, pp. 70–83.
[10] D. Cebon, Assessment of the dynamic wheel forces generated by heavy road vehicles, *Symposium on Heavy Vehicle Suspension and Characteristics*, Austrain Road Research Board, 1987.
[11] A.P. Whittemore, J.R. Wiley, P.C. Schultz, D.E. Pollock, Dynamic pavement loads of heavy highway vehicles, Highway Research Board, *National Cooperative Highway Research Program Report No. 105*, 1970.
[12] R. Cantieni, Dynamic behavior of highway bridges under the passage of heavy vehicles, *Swiss Federal Laboratories for Materials Testing and Research (EMPA) Report No. 220*, 1992.
[13] L. Yu, Accounting for Bridge Dynamic Loads Using Moving Force Identification System (MFIS), PhD Thesis, The Hong Kong Polytechnic University, Hong Kong, 2002.
[14] C. O'Connor, T.H.T. Chan, Dynamic loads from bridge strains, *Journal of Structural Engineering, ASCE* 114 (1988) 1703–1723.
[15] T.H.T. Chan, S.S. Law, T.H. Yung, X.R. Yuan, An interpretive method for moving force identification, *Journal of Sound Vibration* 219 (3) (1999) 503–524.
[16] S.S. Law, T.H.T. Chan, Q.H. Zeng, Moving force identification: a time domain method, *Journal of Sound and Vibration* 201 (1) (1997) 1–22.
[17] S.S. Law, T.H.T. Chan, Q.H. Zeng, Moving force identification: a frequency and time domains analysis, *Journal of Dynamic System, Measurement and Control, ASME* 12 (3) (1999) 394–401.
[18] L. Yu, T.H.T. Chan, Moving force identification based on the frequency–time domain method, *Journal of Sound and Vibration* 261 (2) (2003) 329–349.
[19] L. Yu, T.H.T. Chan, Identification of multi-axle vehicle loads on bridges, *Journal of Vibration and Acoustics, ASME* 126 (1) (2004) 17–26.
[20] T.H.T. Chan, S.S. Law, T.H. Yung, Moving force identification using an existing prestressed concrete bridge, *Engineering Structures* 22 (2000) 1261–1270.
[21] T.H.T. Chan, L. Yu, S.S. Law, Comparative studies on moving force identification from bridge strains in laboratory, *Journal of Sound Vibration* 235 (1) (2000) 87–104.
[22] E.A. Sekhniashvili, I.E. Byus, Y.S. Sarkisov, Work of girder bridge structures under dynamic loads (in Russian), *Beton i zhelezobeton* 11 (1961) 491–494.
[23] Y. Cai, S.S. Chen, D.M. Rote, H.T. Coffey, Vehicle guideway interaction for high-speed vehicles on a flexible guideway, *Journal of Sound and Vibration* 175 (5) (1994) 625–646.
[24] H.P. Lee, Transverse vibration of a Timoshenko beam acted on by an accelerating mass, *Applied Acoustics* 47 (4) (1996) 319–330.
[25] G.T. Michaltsos, Dynamic behavior of a single-span beam subjected to loads moving with variable speeds, *Journal of Sound and Vibration* 258 (2) (2002) 359–372.
[26] S. Sadiku, H.H.E. Leipholz, On the dynamics of elastic systems with moving concentrated masses, *Ingenieur-Archiv* 57 (1987) 223–342.
[27] C. Bilello, L.A. Bergman, D. Kuchma, Experimental investigation of a small-scale bridge model under a moving mass, *Journal of Structural Engineering, ASCE* 130 (5) (2004) 799–804.
[28] A.V. Pesterev, L.A. Bergman, Response of elastic continuous carrying moving linear oscillator, *Journal of Engineering Mechanics, ASCE* 123 (8) (1997) 878–884.
[29] B. Yang, C.A. Tan, L.A. Bergman, Direct numerical procedure for solution of moving oscillator problems, *Journal of Engineering Mechanics, ASCE* 126 (5) (2000) 269–462.
[30] K.B. Todd, B.T. Kulakowski, Simple computer models for predicting ride quality and loading for heavy trucks, *Transportation Research Record*, 1215, TRB, National Research Council, Washington, DC, 1989.
[31] P.K. Chatterjee, T.K. Datta, C.S. Surana, Vibration of suspension bridges under vehicular movement, *Journal of Structural Engineering, ASCE* 120 (3) (1994) 681–703.
[32] G. Lindfield, J. Penny, *Numerical Method using MATLAB*, Ellis Horwood Limit, London, 1995.
[33] AASHTO, *Standard Specification for Highway Bridges*, American Association of State Highway and Transportation, Washington, DC, USA, 1996.
[34] T.H.T. Chan, L. Yu, S.S. Law, T.H. Yung, Moving force identification studies II: comparative studies, *Journal of Sound and Vibration* 247 (1) (2001) 77–95.
[35] Y.B. Yang, J.D. Yau, Vehicle–bridge interaction element for dynamic analysis, *Journal of Structural Engineering, ASCE* 123 (11) (1997) 1512–1518.
[36] T.H.T. Chan, L. Yu, S.S. Law, T.H. Yung, Moving force identification studies I: theory, *Journal of Sound and Vibration* 247 (1) (2001) 59–76.
[37] L. Yu, T.H.T. Chan, Moving force identification from bending moment responses of bridge, *Structural Engineering and Mechanics* 14 (2) (2002) 151–170.

[38] A.N. Tikhonov, V.Y. Arsenin, *Solution of Ill-posed Problems*, Wiley, New York, 1977.
[39] S.S. Law, T.H.T. Chan, X.Q. Zhu, Q.H. Zeng, Regularization in moving force identification, *Journal of Engineering Mechanics, ASCE* 127 (2) (2001) 136–148.
[40] H.R. Busby, D.M. Trujillo, Optimal regularization of an inverse dynamics problem, *Computers and Structures* 63 (2) (1997) 243–248.
[41] P.C. Hansen, Analysis of discrete ill-posed problems by means of the *L*-curve, *SIAM Review* 34 (4) (1992) 561–580.
[42] T.H.T. Chan, T.H. Yung, A theoretical study of force identification using prestressed concrete bridge, *Engineering Structures* 23 (2000) 529–1537.
[43] H.G. Harris, G.M. Sabnis, *Structural Modeling and Experimental Techniques*, CRC Press, New York, 2000.
[44] R.T. Wang, Y.L. Sang, Out-of-plane vibration of multi-span curved beam due to moving loads, *Structural Engineering and Mechanics* 7 (4) (1999) 361–375.
[45] M.A. Khaleel, R.Y. Itani, Live-load moments for continuous skew bridges, *Journal of Structural Engineering, ASCE* 116 (9) (1990) 2361–2373.
[46] R.J. Jiang, F.T.K. Au, Y.K. Cheung, Identification of masses moving on multi-span beams based on a genetic algorithm, *Computers and Structures* 81 (2003) 2137–2148.
[47] F.T.K. Au, R.J. Jiang, Y.K. Cheung, Parameter identification of vehicles moving on continuous bridges, *Journal of Sound and Vibration* 269 (2004) 91–111.
[48] C.R. Vogel, J.G. Wade, Iterative SVD-based methods for ill-posed problems, *SIAM Journal on Scientific Computing* 15 (1994) 736–754.
[49] F.S.V. Bazan, C.A. Bavaseri, An optimized pseudo-inverse algorithm (OPIA) for multi-input multi-output modal parameter identification, *Mechanical Systems and Signal Processing* 10 (4) (1996) 365–380.
[50] W.X. Zhong, F.W. Williams, A precise time step integration method, *Proceedings of Institution of Mechanical Engineers, Part C: Journal of Mechanical Engineering Science* 208 (1994) 427–430.
[51] X.Q. Zhu, S.S. Law, Practical aspects in moving force identification, *Journal of Sound and Vibration* 258 (1) (2002) 123–146.
[52] Y. Mitsuhata, Adjustment of regularization in ill-posed linear inverse problems by the empirical Bayes approach, *Geophysical Prospecting* 52 (2004) 213–239.
[53] D. Watzenig, B. Brandstatter, G. Holler, Adaptive regularization parameter adjustment for reconstruction problems, *IEEE Transactions on Magnetics* 40 (2) (2004) 1116–1119.
[54] L.C. Chu, N.S. Qu, R.F. Wu, A forward method for dynamic load identification in time domain, *Chinese Journal of Applied Mechanics* 11 (2) (1994) 9–18.
[55] L.J.L. Nordstrom, T.P. Nordberg, A time delay method to solve non-collocated input estimation problems, *Mechanical Systems and Signal Processing* 18 (2004) 1469–1483.
[56] T.H.T. Chan, T.H. Yung, Identification of bridge-friendly vehicles from different vehicle frames, *Proceedings of the International Conference on Advances in Structural Engineering*, Hong Kong, 13–15 December 2000, pp. 577–584.